EUROPHYSICS LETTERS

OFFPRINT

Vol. 72 • Number 4 • pp. 569–575

Site preference of hydrogen in metal, alloy, and intermetallic frameworks

* * *

P. Vajeeston, P. Ravindran, R. Vidya, A. Kjekshus and H. Fjellvåg

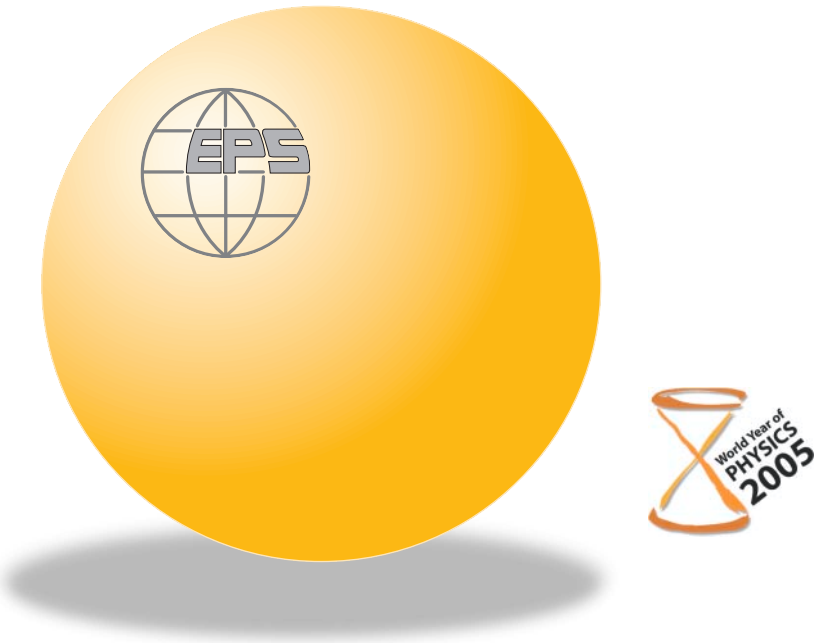

Published under the scientific responsability of the
EUROPEAN PHYSICAL SOCIETY
Incorporating
JOURNAL DE PHYSIQUE LETTRES • LETTERE AL NUOVO CIMENTO

EUROPHYSICS LETTERS 15 November 2005

Europhys. Lett., **72** (4), pp. 569–575 (2005)
DOI: 10.1209/epl/i2005-10280-2

Site preference of hydrogen in metal, alloy, and intermetallic frameworks

P. Vajeeston, P. Ravindran, R. Vidya, A. Kjekshus and H. Fjellvåg
Department of Chemistry, University of Oslo - Box 1033 Blindern, N-0315 Oslo, Norway

received 5 August 2005; accepted in final form 21 September 2005
published online 14 October 2005

PACS. 61.50.Ah – Theory of crystal structure, crystal symmetry; calculations and modeling.
PACS. 61.50.Lt – Crystal binding; cohesive energy.
PACS. 71.15.Nc – Total energy and cohesive energy calculations.

Abstract. – To design new hydrogen storage materials a main prerequisite is the knowledge about the site preference of hydrogen in the corresponding nonhydride phases. From the systematic investigation of ZrNiAl-type phases we found that the electron-localization function (ELF) can correctly predict the site preference of hydrogen in metallic phases. From the site preference trends of H in ZrNiAl-type phases we have shown that hydrogen prefers to occupy interstitial sites where ELF indicates a maximum value. Based on this observation we generalized an empirical site-preference rule which states that hydrogen prefers to occupy the interstitial sites where electrons have relatively more nonbonding localized nature than other possible sites in metals, alloys and intermetallic frameworks.

Hydrogen is considered as one of the best alternative fuels due to its abundance, easy synthesis, and non-polluting nature. For the on-board energy storage in vehicles one needs hydrogen storage materials with high gravimetric and volumetric densities of hydrogen. In order to achieve the high volumetric density of hydrogen, it is important to find potential materials where one can pack hydrogen atoms or molecules more efficiently. There are several hydrides identified recently [1, 2] where the gravimetric and volumetric density of hydrogen is sufficiently larger. However, the sorption kinetics of hydrogen in such materials are very poor. So, we require a more detailed knowledge about the interaction of hydrogen with the host matrices in order to design potential hydrogen storage materials for future applications.

The shortest H–H separation between two hydrogen atoms in a crystalline framework is limited by the H-to-H repulsion and it is commonly believed that two hydrogen atoms cannot be located closer together than some 2.0 Å [3]. This so-called "2-Å rule" appears to hold for the absolute majority of precisely described structures of metal (alloy/intermetallic) hydrides. However, the structural knowledge for hydrides is by and large very limited owing to complexity in structural arrangements and difficulties involved in establishing hydrogen positions. A recent experimental study [4] on RNiIn (R = La, Ce, Nd; generally a rare-earth element) series shows that hydrides of these compounds violate the "2-Å rule" vigorously. Using density functional calculations we have explained [5, 6] the origin for the violation and suggested that the H–H separation may be reduced to even below 1.5 Å by combinations of other element. The RNiIn phases crystallize in the ZrNiAl-type structure (fig. 1), which

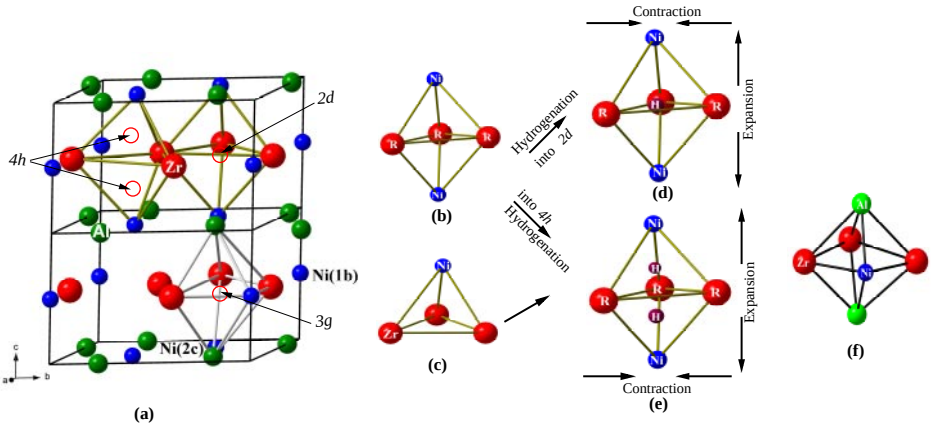

Fig. 1 – (Color online) (a) The ZrNiAl-type crystal structure (RTM). Legends for the different kinds of atoms are given in the illustration. The $2d$ (trigonal-bipyramidal interstice), $4h$ (tetrahedral interstice), and $3g$ (distorted octahedral interstice) sites are indicated by open circles and pointed by arrows. (b) The empty trigonal-bipyramidal interstice. (c) The empty tetrahedral interstice. (d) The trigonal-bipyramidal interstice filled with hydrogen. (e) Two face-sharing tetrahedral interstices filled with hydrogen. (f) The empty (distorted) octahedral interstice.

comprises a family of more than 300 individuals [7] and only few of the hydrides of these compounds are identified experimentally.

The electron-localization function (ELF) is a useful tool to characterize chemical bonding in solids. For example, Savin *et al.* [8] distinguished different kinds of bonding in a wide range of materials and also demonstrated that it is possible to identify the site preference for hydrogen in the Ca metal using ELF analysis. ELF is a measure for the probability distribution of paired electrons, and this function is able to better distinguish different bonding situations for electrons than the plain charge-density distribution [9]. For example, it is usually hard [8, 9] to distinguish $K, L, M, \ldots$ core shells from inspection of charge-density distributions whereas ELF can discriminate individual shells and disclose details in their electron distributions. Using ELF analysis we show that H atoms in metal matrices prefer to enter interstitial sites which have more nonbonding localized electrons than the other sites.

The theoretical simulations have utilized the DFT with plane-wave basis sets using the Vienna *ab initio* simulations package (VASP) [10], which calculates the Kohn-Sham ground state via an iterative band-by-band matrix-diagonalization scheme and charge-density mixing [10]. All calculations employed the generalized-gradient approximation (GGA) of Perdew and Wang [11]. The valence electrons were explicitly represented with projector-augmented plane-wave (PAW) [12] pseudopotentials. Theoretical simulations have been performed with full geometry optimization and without any constrains where the ions are relaxed toward equilibrium until the Hellmann-Feynman forces are less than 10^{-3} eV/Å. Brillouin zone integration is performed with a Gaussian broadening of 0.1 eV during all relaxations. All calculations are performed with 768 $\boldsymbol{k}$ points in the whole Brillouin zone and a 600 eV plane-wave cutoff. The preference for hydrogen localization in the $2d$ and $4h$ sites of space group $P\overline{6}2m$ with full occupancy have been systematically tested for the considered ZrNiAl-type phases (more surveying studies have been made for the $3g$ site). Equilibrium volumes and unit-cell parameters were extracted from calculated energy *vs.* volume data by fitting to the "universal equation of state" proposed by Vinet *et al.* [13]. The hydride-formation energy (ΔE) was calculated

TABLE I – *Optimized unit-cell dimensions (in* Å*) and positional parameters, hydrogen-formation energy (in* kJ/mol*), and shortest* H–H *separation (in* Å*) for selected* ZrNiAl*-type phases (space group* $P\bar{6}2m$*; sites: R in* $3g$ $(x, 0, 1/2)$*, T in 1b* $(0, 0, 1/2)$ *and 2c* $(1/3, 2/3, 0)$*, and M in* $3f$ $(x, 0, 0)$*; for hydrogen: 2d* $(2/3, 1/3, 1/2)$*, 4h* $(1/3, 2/3, z)$*, and 3g* $(x, 0, 1/2)$*).*

Compound	Unit cell (a and c)	Positional parameters	$-\Delta E$	H–H separation
ZrNiAl	6.8738 (6.9152)[a] 3.5652 (3.4703)[a]	R: $x = 0.5904$ (0.591)[a]; M: $x = 0.2482$ (0.251)[a]		
$ZrNiAlH_{0.666}$	6.8651 (6.7225)[a] 3.6579 (3.7713)[a]	R: $x = 0.5947$ (0.592)[a]; M: $x = 0.2477$ (0.246)[a] H($2d$)	46.59	3.77
LaNiIn	7.6046 (7.5906)[b] 4.0850 (4.0500)[b]	R: $x = 0.5866$ (0.5940)[b]; M: $x = 0.2475$ (0.256)[b]		
$LaNiInH_{1.333}$	7.3853 (7.3810)[b] 4.6761 (4.6489)[b]	R: $x = 0.6036$ (0.6035)[b]; M: $x = 0.2444$ (0.2437)[b] H($4h$): $z = 0.6728$ (0.6759)[b]	46.26	1.63 (1.64)
$LaNiInH_{2.333}$	7.3828 (7.3874)[c] 4.8436 (4.6816)[c]	R: $x = 0.5982$ (0.603)[c]; M: $x = 0.2547$(0.247)[c] H($4h$): $z = 0.3182$ (0.317)[c]; H($3g$): $x = 0.2193$ (0.226)[c]	35.04	1.75 (1.72)
ThCoAl	7.1711 (7.0460)[d] 4.0313 (4.0364)[d]	R: $x = 0.5861$; M: $x = 0.2266$		
$ThCoAlH_{1.333}$	7.0854 4.3207	R: $x = 0.6124$; M: $x = 0.2399$ H($4h$): $z = 0.6620$	10.322	1.40
ThNiIn	7.3815 (7.3673)[d] 4.1690 (4.1170)[d]	R: $x = 0.5835$; M: $x = 0.2443$		
$ThNiInH_{1.333}$	7.1519 4.3664	R: $x = 0.6008$; M: $x = 0.2514$ H($4h$): $z = 0.6658$	28.09	1.45
YNiIn	7.4536 (7.4860)[d] 3.8272 (3.7840)[d]	R: $x = 0.5890$; M: $x = 0.2536$		
$YNiInH_{0.666}$	7.4611 3.8182	R: $x = 0.5912$; M: $x = 0.2539$ H($2d$)	64.36	3.72

[a] Experimental value from ref. [15].
[b] Experimental value from ref. [16].
[c] Experimental value from ref. [16] with D in $4h$ (96% occupancy) and $3g$ (36% occupancy).
[d] Experimentalvalue from ref. [7].

from the relation

$$\Delta E = \frac{1}{x}[E(RTMH_x) - E(RTM)] - \frac{1}{2}E(H_2), \tag{1}$$

where x refers to the hydrogen content per formula unit (*viz* $x = 0.667$, 1.333 or 2.333 for the filled-up site(s) under consideration), T is a transition metal, M an element in the periodic table, $E(RTMH_x)$ represents the energy of the hydride phase, $E(RTM)$ the energy of the intermetallic phase, and $E(H_2)$ the energy of the dihydrogen molecule (−6.795 eV).

It should be noted that in the VASP code no corrections for local augmentation functions are applied during the ELF calculation. This may have noticeable effect on the calculated ELF values. In order to clarify this effect we have compared the calculated ELF results obtained from TBLMTO and VASP codes. Both yielded almost the same qualitative features except a shift in the magnitude of the ELF value. In this present study we are mainly concentrating on the qualitative features rather than on the absolute value. Hence, the main conclusion of the present work may not be affected by the ELF value obtained from the VASP code.

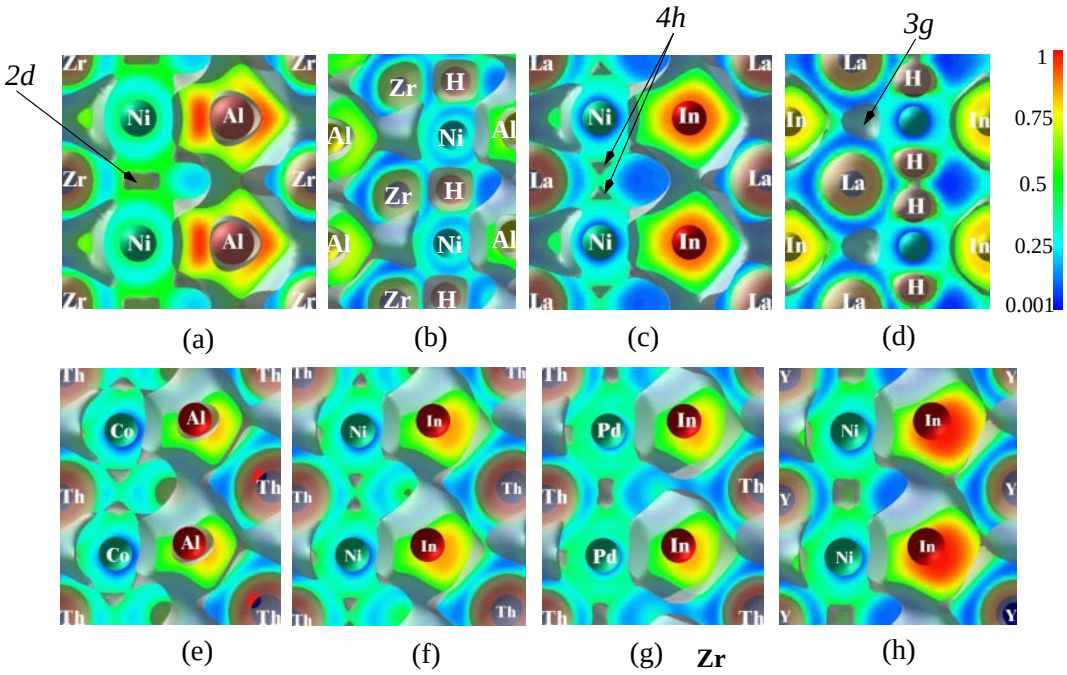

Fig. 2 – (Color online) Calculated ELF in the (001) plane for (a) ZrNiAl, (b) $ZrNiAlH_{0.667}$, (c) LaNiIn, (d) $LaNiInH_{1.333}$, (e) ThCoAl, (f) ThNiIn, (g) ThPdIn, and (h) YNiIn. Different crystallographic sites ($2d$, $4h$, and $3g$) are marked by arrows. The iso-surface values correspond to 0.6 ELF value. Legends for the different kinds of atoms are given in the illustration.

The ZrNiAl-type structure (see fig. 1 and table I; maintaining the general formula RTM) has eight different interstitial sites centered around $2d$, $2e$, $3f$, $3g$, $4h$, $6i$, $6k$, and $12l$. Of these, the tetrahedral holes around $4h$ (surrounded by $3R$ and $1T$), the trigonal-bipyramidal holes around $2d$ (surrounded by $3R$, $1T$, and $1M$), and the distorted octahedral holes around $3g$ (surrounded by $3R$, $1T$, and $2M$) are the most interesting in relation to hole size [14] and symmetry. We have searched the site preference of hydrogen in all these possible interstitial sites for around a hundred ZrNiAl-type compounds. Even though we have examined a large number of ZrNiAl-type phases, it is convenient to concentrate the presentation of the findings on two typical examples, where hydrogen prefers to occupy different sites.

The hole size for all interstitial sites of the ZrNiAl structure (as derived from structural parameters [15] and atomic radii) shows that the $2d$ and $12l$ sites give rise to the largest interstitial holes; radius 0.49 and 0.43 Å, respectively. The experimental study [15] showed that hydrogenation of ZrNiAl leads to $ZrNiAlH_{0.53}$, with the hydrogen atoms on the $2d$ site. The theoretically optimized structural parameters for the ZrNiAl matrix came out in very good agreement with the experimental values (table I). In order to locate possible hydrogen positions in the hydride phase, the ELF for ZrNiAl was systematically visualized in different planes. The results showed that electrons only have a tendency to accumulate at the $2d$ site (fig. 2a; ELF above 0.6 at the $2d$ site and much smaller values at the other interstitial sites). Hydrogen with full occupancy was subsequently placed in the $2d$ site and atomic positions as well as unit-cell parameters were optimized. The thus obtained optimized structural parameters fit very well with the experimental data (within the 3% limit typical for DFT calculations).

Calculations performed on the assumption of accommodation of hydrogen in the other interstitial sites gave poorer fits to the experimental values and less favorable hydride-formation energies. The shortest H–H separation in the $ZrNiAlH_{0.667}$ phase obeys the "2-Å rule".

Exactly the same approach has been used systematically to identify hydrogen positions in the isotypic LaNiIn phase. Hole-size considerations for the experimental structural parameters of LaNiIn [16] suggest that $3g$ (hole radius 0.63 Å), $4h$ (0.47 Å), and $3f$ (0.45 Å) are the possible interstitial sites for the accommodation of hydrogen. First, we have optimized the structural parameters for LaNiIn and the calculated parameters are found to be in good agreement with the experimental findings (table I). Using the theoretically optimized structural parameters we have derived the ELF and visualized this function in different planes of the LaNiIn structure. Inspection of these ELF maps revealed that nonbonding localized electrons are accumulated at the $4h$ site (ELF above 0.6 at the $4h$ site and negligible ELF at all other interstitial sites; fig. 2c). The subsequent structural optimization for the corresponding filled-up $LaNiInH_{1.333}$ structure shows that this is indeed a very likely atomic arrangement for the hydride, with again quite good agreement between experimental and theoretical structural variables (table I). It is worthwhile noting that calculations based on accommodation of hydrogen in the other interstitial sites gave also in this case poorer fit to the experimental data and less favorable hydride-formation energies. Like the ZrNiAl-to-$ZrNiAlH_{0.667}$ conversion, the hydrogenation of LaNiIN to $LaNiInH_{1.333}$ causes highly anisotropic lattice changes; contraction of a and expansion of c. It should be noted that $ZrNiAlH_{0.667}$ obeys the 2-Å rule whereas $LaNiInH_{1.333}$ violates it (see table I).

It is clear from our ELF analysis that compared to the crystal structure the chemical environment around a given interstitial site plays a decisive role to accommodate hydrogen. On this background it is interesting to visualize the ELF for $LaNiInH_{1.333}$ (see fig. 2d) to look for possible interstitial sites where hydrogen prefers to occupy. With the $4h$ site filled up by hydrogen, another interstitial site ($3g$) with an ELF value of around 0.6 appears (while other interstitial sites still show negligible ELF levels). A recent study of deuteriation of LaNiIn under pressure ($p_{D_2} = 4.6$ bar) has revealed a new phase, $LaNiInD_{1.64}$, in which deuterium occupies both the $4h$ (96% filled) and $3g$ (36% filled) sites. The structural optimization for the corresponding filled-up $LaNiInH_{2.333}$ structure gave unit-cell dimensions and positional parameters in satisfactory agreement (*viz* within the expected accuracy for DFT calculations) with the experimental findings for $LaNiInD_{1.64}$ (table I). The effect of partial *vs.* full occupancy of hydrogen positions appears to be of subordinate importance for the structural details. The formation energy for hydrogenation from $LaNiInH_{1.333}$ to $LaNiInH_{2.333}$ (table I) confirms that this conversion is thermodynamically acceptable as already demonstrated by experiment. As a consistency check, structural optimizations and formation-energy estimates were also made for other combinations of fully occupied interstitial sites. The outcome (table I) confirms that the interstitial site combination $4h$ and $3g$ is the only realistic possibility in this case. Inspired by the ability of ELF to predict the existence of $LaNiInH_{2.333}$, ELF maps were prepared for $ZrNiAlH_{0.667}$. However, additional sites with nonbonding electron localization did not show up in the ELF maps (see fig. 2b) and calculations of formation energies (positive ΔE; not documented) confirm that $ZrNiAlH_{0.667}$ should be the most hydrogen-rich phase in ZrNiAl.

It was indeed the success of ELF to correctly predict the site preference of hydrogen in the just discussed hydride phases that led us to undertake a more systematic study of the ZrNiAl-type family. The working hypothesis was that when the ELF at a certain interstitial site takes a maximum that exceeds 0.5, then this site will favor accommodation of hydrogen. The ELF criterion predicts that hydrogen prefers the $2d$ site for 43% of the studied RTM phases (*e.g.*, YNiIn (see fig. 2h), ThRhSn, and ZrCoGa) and the $4h$ site for 12% (*e.g.*, CeNiIn, PrNiIn, and NdNiIn). For 5% of the RTM phases (*e.g.*, ThPdIn (see fig. 2g), ScMnSi, and

ThNiGa) the ELF is unable to provide a clear-cut distinction between the 2*d* and 4*h* sites. The ELF for these phases is generally blurred in the interstitial regions and the ELF level at 2*d* and 4*h* sites reflects a more even charge distribution. For 40% of the studied *RTM* phases (*e.g.*, ZrAsOs, ScPdGe, and ThIrAl) the ELF predicts that any attempted hydrogenation would be unsuccessful. These predictions compare reasonably well with the corresponding calculated formation energies, which show that 44% of the 95 examined *RTM* phases have a clear preference for the 2*d* site, 10% for the 4*h* site, 8% undecided, and 38% unamendable for hydrogen. Table I includes predicted crystal-structure and formation-energy data for three, more or less arbitrarily chosen hydride phases based on the ZrNiAl-type matrix. Figures 2e-f show the ELF illustrations for ThCoAl, ThNiAl, and YNiIn. The above selection of ZrNiAl-type phases should permit a first experimental check of the predicting power of what we would like to propose as a *site-preference rule* for hydrogen in metal matrices: *Hydrogen prefers to occupy the interstitial sites where electrons have relatively more nonbonding localized nature than other possible sites in metals, metal matrices and intermetallic frameworks.*

Finally, a few words about the origin of the site-preference rule. The maximum value of ELF (more than 0.5) in a particular interstitial site indicates that the chemical environment in that place is such that those electrons have relatively more paired nature (*i.e.* nonbonding localized electrons) than other interstitial sites. When hydrogen atom is diffused into the metal matrices it has one unpaired electron. The diffused hydrogen with one unpaired electron will try to find a place in the metal matrix where it can find electrons that can easily participate in the bonding interaction such that it can achieve a more stable $1s^2$ paired electron configuration and thereby completes its valence shell. The maximum value of ELF (more than 0.5) in the interstitial regions indicates that nonbonding localized electrons at those regions can more easily go to the H sites than electrons from other interstitial sites. This is the physical origin for the site preference of H in interstitial sites where ELF has the maximum value. Another mechanism for such a process is that a hydrogen atom on entering the interior of the metal matrix gives up its own electron to the collective interstitial electron well (thus forming an H^+ ion (*viz* a bare proton)), undergoes lattice diffusion, and arranges itself on an appropriate interstitial site with high ELF, where it attracts nonbonding localized electrons and establishes a paired state. The net outcome of the two processes is the same, H gains one electron from the host lattice and establishes H^- with a paired s^2 state. This complies with our finding that charge-transfer plots in metal hydrides always show electron transfer from the host lattice to H. The higher ELF values in certain interstitial regions signal that electrons in these regions have appropriate spin available for completion of the valence shell of the incorporated hydrogen atoms. If more than one interstitial sites show large nonbonding localized electrons in a particular matrix, it seems likely that first hydrogen atoms will go to the site with the largest amount of nonbonding localized electrons. As a result of the filling of this site, electron localization on other sites may either increase or decrease. In the former case a new site may be available for hydrogen filling, say, when exposed to high hydrogen pressures.

* * *

The authors gratefully acknowledge the Research Council of Norway for financial support and for the computer time at the Norwegian supercomputer facilities.

REFERENCES

[1] Züttel A., *Mater. Today*, **24**, September issue (2003).
[2] Seayad A. M. and Antonelli D. M., *Adv. Mater.*, **16** (2004) 765.

[3] Switendick A. C., *Z. Phys. Chem.*, **117** (1979) 89.
[4] Yartys V. A., Denys R. V., Hauback B. C., Fjellvåg H., Bulyk I. I., Riabov A. B. and Kalychak Ya. M., *J. Alloys Compounds*, **330-332** (2002) 132.
[5] Ravindran P., Vajeeston P., Vidya R., Kjekshus A. and Fjellvåg H., *Phys. Rev. Lett.*, **89** (2002) 106403.
[6] Vajeeston P., Ravindran P., Fjellvåg H. and Kjekshus A., *Phys. Rev. B*, **70** (2004) 014107.
[7] Villars P. and Calvert L. D. (Editors), *Pearson's Handbook of Crystallographic Data for Intermetallic Phases*, 2nd edition (American Society for Metals, Materials Park, OH) 1986.
[8] Savin A., Nesper R., Wengert S. and Fässler T. F., *Angew. Chem. Int. Ed. Engl.*, **36** (1999) 1808.
[9] Kohout M. and Savin A., *J. Comput. Chem.*, **18** (1997) 1431.
[10] Kresse G. and Hafner J., *Phys. Rev. B*, **47** (1993) R6726.
[11] Perdew J. P., Burke V. and Wang Y., *Phys. Rev. B*, **54** (1996) 16533.
[12] Blöchl P. E., *Phys. Rev. B*, **50** (1994) 17953.
[13] Vinet P., Ferrante J., Smith J. R. and Rose J. H., *J. Phys. C*, **19** (1986) L467.
[14] Westlake D. G., *J. Less-Common Met.*, **103** (1984) 203.
[15] Yoshida M., Akiba E., Shimojo Y., Morii Y. and Izumi F., *J. Alloys Compounds*, **231** (1995) 755.
[16] Denys R. V., Riabov A. B., Yartys V. A., Hauback B. C. and Brinks H. W., *J. Alloys Compounds*, **356-357** (2003) 65.